How do mobility restrictions and social distancing during COVID-19 affect oil price?

Asim K. Dey[1,2] · Kumer P. Das[3]

Abstract

This paper provides an analysis of the effect of the COVID-19 outbreak on the crude oil price. Using a newly developed air mobility index and Apple's driving trends index, we assess the effect of human mobility restrictions and social distancing during the COVID-19 pandemic on the crude oil price. We apply a quantile regression model, which evaluates different quantiles of the crude oil price. We also conduct an extreme value modeling, which examines the lower tail of the crude oil price distribution. We find that both the air mobility index and driving trends index significantly influence lower and upper quantiles of the WTI crude oil price. The extreme value models suggest that there is a potential risk of a negative crude oil price for a sudden extreme fall of air mobility.

Keywords COVID-19 · Oil price · Apple mobility trends · Airline complex network · Granger causality · Quantile regression · Extreme value theory

1 Introduction

Understanding the real-time fuel demand is very important for many reasons. Energy merchants want to get a trading edge from all possible resources such as thermal images from cameras on pipelines, satellite data tracking worldwide oil tankers, and so on. Another way of quantifying the real-time demand is by tracking the transportation sector which accounts for the largest share of US petroleum consumption. In 2019,

✉ Kumer P. Das
  kumer.das@louisiana.edu

  Asim K. Dey
  adey@utep.edu

1 Department of Mathematical Sciences, University of Texas at El Paso, El Paso, TX, USA

2 Department of Electrical and Computer Engineering, Princeton University, Princeton, NJ, USA

3 The Office of Vice President for Research, Innovation, and Economic Development, University of Louisiana at Lafayette, Lafayette, LA, USA

the transportation sector accounts for 68% of all petroleum consumption in the USA. Moreover, finished motor gasoline accounts for about 45% of total US petroleum consumption (US Energy Information Administration). Human mobility trends introduced by Apple Inc. [2] in mid-April can also be used to understand on-the-spot gasoline consumption data as it captures user activity in searching for directions on smartphones.

In the last one year, many projects have been developed to assess the effect of the COVID-19 pandemic on the oil price. Corbet et al. (2020) [42] analyze volatility spillovers and volatility co-movements among energy-producing, extracting, and transporting corporations' stock prices over and evaluate how the COVID-19 pandemic creates negative WTI oil price. Akhtaruzzaman et al. [78] and Mugaloglu et al. [79] investigate different financial oil price risk exposure during the COVID'19 pandemic. Narayan (2020) evaluate the importance of COVID-19 infections and oil price news in influencing oil price. In the last several years an increasing number of studies have also been undertaken to evaluate different determinants, of crude oil price. Among such recent results, Ratti and Vespignani (2016) [34], Kollias et al. (2013) [73], and Colgan (2013) [71] analyze the effect of supply, demand, and geopolitical events on the crude oil price. Dey et al. (2020) [13] evaluate the effect of supply, demand, and geopolitical events on extreme crude oil price based on a non-stationary extreme value model.

Indeed, one of the key determinants of crude oil price is demand, and crude oil demand is highly influenced by human mobility. Since the outbreak of the COVID-19 pandemic, governments and officials have been implementing containment measures aimed at reducing the spread of the virus, including social distancing and restrictions to human mobility. However, there is no study has been conducted on how mobility restrictions and social distancing during COVID-19 influence crude oil price. In this paper, we introduce and formalize the notion of *temporal airline network* to understand the impact of mobility restrictions and social distancing on airline flight volumes. A larger flight volume corresponds to higher oil demand. We develop an air mobility index based on the number of edges of an airline network to evaluate the dynamics of daily US flight volumes. We also use the Apple driving index [2] to quantify driving trends during the COVID-19 pandemic. A low score of the two indices indicates that people follow the government's guidelines on mobility restrictions more and practice more social distancing. Conversely, a high score of the two indices implies lower mobility restrictions and less social distancing.

The objective of this study is to understand the impact of the Apple *driving trend index* and the newly developed *air mobility index* on the crude oil price. For this purpose, first, we evaluate the Granger causality of driving trends and air mobility on the crude oil price. Second, we investigate the effect of driving trends and air mobility on the different quantiles of the crude oil price based on the quantile regression model. Third, we assess the tail of the crude oil price using an extreme value model. Generally, extreme value models focus on the upper tail of the distribution. However, we study the lower tail of the crude oil price and analyze different determinants of extreme lower crude oil price based on non-stationary extreme value model as discussed in Dey et al. (2020) [13].

The rest of the paper is organized as follows. In Sect. 2 we introduce different measures of mobility restrictions and social distancing. In Sect. 3 we describe the data. We discuss the two methods, namely, quantile regression and extreme value theory, used in the study in Sect. 4. We report the findings and describe the results in Sect. 5. Finally, we conclude in Sect. 6.

2 Quantification of Mobility Restrictions and Social Distancing

To control the spread of COVID-19 different governments have been implementing a variety of mobility restrictions and social distancing measures [8, 20, 32, 37]. To quantify the impact of such control measures on human mobility behavior we utilize the two following mobility indices.

2.1 Apple's Driving Trend Index

The Apple driving trend represents a relative driving volume of Apple users compared to a baseline volume on January 13, 2020. Our study considers a weekly average of the Apple driving trend between January 13, 2020, and August 25, 2020, as a measure of mobility. We name this measure as *Apple driving trend index* (ADI). We normalize ADI in week t by adjusting the average ADI and corresponding standard deviation as

$$H_t = \frac{ADI_t - \mu_{ADI}}{\sigma_{ADI}}, \tag{1}$$

where μ_{ADI} and σ_{ADI} are the mean and standard deviation of ADI between January 13, 2020, and August 25, 2020.

2.2 Air Mobility Index

In our study, we consider daily flight volumes in the USA as a measure of air mobility. To evaluate daily flight volumes, we introduce a complex network analysis. We define a graph $G = (V, E)$ as a model for an airline network, with node set V and set of edges $E \subset V \times V$ such that $(u, v) \in E$ represents an edge from node u to v, $u, v = 1, 2, \cdots, n$. Here, the nodes represent the US airports and if there is a direct flight between two nodes (i.e., airports) they are connected by an edge. Here $|V|$ is the number of nodes and $|E|$ is the number of edges in the network. The elements of the $n \times n$-symmetric *adjacency matrix*, A, of G can be written as

$$A_{ij} = \begin{cases} 1, & \text{if } (i, j) \in E \\ 0, & \text{otherwise.} \end{cases} \tag{2}$$

We assume that G is *undirected*, i.e., for all $e_{uv} \in E$, $e_{uv} \equiv e_{vu}$.

(a) US airline network on Feb 2, 2020.   (b) US airline network on May 3, 2020.
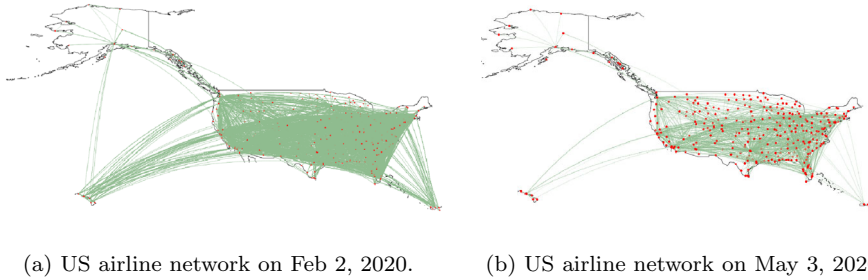
Fig. 1 Impact of COVID-19 on US airlines. Red points represent nodes (airports) and green lines represent edges. **a** Shows normal US airline network with 340 nodes and 18,805 edges. **b** Represents reduced US airline network with 319 nodes and 4,980 edges

A temporal network is a network structure that changes in time, which can be represented with a time indexed graph $G^t = (V(t), E(t))$, where, $V(t)$ is the set of nodes in the network at time t, $E(t) \subset V(t) \times V(t)$ is a set of edges in the network at time t [12, 14, 19]. Here, t is either discrete or continuous. To quantify the impact of COVID-19 on flight volumes which necessarily determines the jet fuel demand, we construct two temporal airline network (G^t) for two different time scales. First, we develop a weekly airline network (G_w^t) in each week Sunday day (t) between January 13, 2020, and August 25, 2020: $\mathbb{G}_w = \{G_w^1, \ldots, G_w^{\mathcal{T}}\}$, where $\mathcal{T} = 32$. We consider the airline network on each Sunday is an average representation of that week. The number of nodes $(|V_t^w|)$, number of edges $(|E_t^w|)$, and degree distribution are evaluated in each G_w^t. Figure 1 illustrates the US flight volumes on Feb 2, 2020, and on May 3, 2020.

Second, we construct a monthly airline network (G_m^t) on 15th of each month (t) between January 2000 and August 2020: $\mathbb{G}_m = \{G_m^1, \ldots, G_m^{\mathcal{T}}\}$, where $\mathcal{T} = 248$. We consider the airline network on 15th of each month is an average representation of that month. Similarly as $\mathbb{G}_w$, we evaluate the number of nodes $(|V_t^m|)$, number of edges $(|E_t^m|)$, and degree distribution in each G_m^t.

In our study, we consider the number of edges in an airline network at time t as a measure of air mobility. We name the metrics as *air mobility index* (AMI). Therefore, we define the weekly and monthly air mobility index as $AMI_t^w = |E_t^w|$ and $AMI_t^m = |E_t^m|$, respectively. Similar to Eq. 1, we normalize AMI^w and AMI^m as

$$K_t^w = \frac{AMI_t^w - \mu_{AMI^w}}{\sigma_{AMI^w}} \quad \text{and} \quad K_t^m = \frac{AMI_t^m - \mu_{AMI^m}}{\sigma_{AMI^m}}, \qquad (3)$$

where μ_{AMI^w}, μ_{AMI^m} and σ_{AMI^w}, σ_{AMI^m} are the mean and standard deviation of AMI^w and AMI^m, respectively.

2.3 COVID-19 and Mobility Trend

We study the impact of COVID-19 variables (**C**), e.g., weekly US new cases, weekly US new deaths on US mobility dynamics, and social distancing. We standardized each
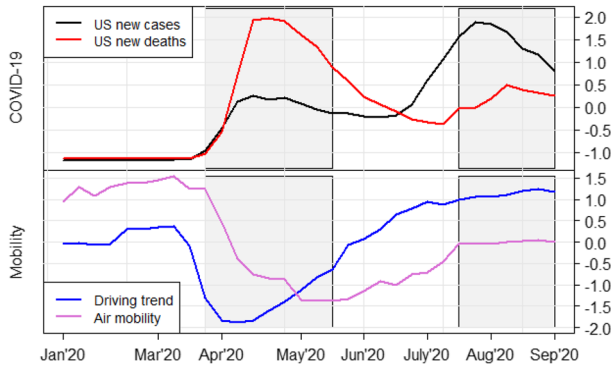
Fig. 2 Time plots of normalized weekly average of COVID-19 variables (new cases and new deaths in the USA) and normalized weekly average mobility metrics from January 2020 to September 2020

COVID-19 variable as

$$O_t = \frac{C_t - \mu_C}{\sigma_C}, \tag{4}$$

where C_t is a COVID-19 variable (weekly US new cases, weekly US new deaths) in week t, μ_C and σ_C are the mean and standard deviation of the corresponding variable between January 13, 2020, and August 25, 2020.

Figure 2 shows the time plots of the normalized weekly average of COVID-19 new cases and deaths in 2020, along with the two mobility indices, i.e., weekly driving trend and weekly air mobility in 2020. Notice that in the first gray region, between late March and middle of May, when the COVID-19 new cases and deaths jump, the driving trends and air mobility collapse. However, in the second gray region, between the middle of July and the end of August, even though there are surges in new cases and deaths, driving trend and air mobility increase gradually. That is, initially a sudden increase in COVID-19 new cases and deaths negatively influence the driving trend and air mobility, but after a certain period, high COVID-19 new cases and deaths do not cause lower driving and decrease air mobility.

3 Data

The WTI crude oil price ($ per Barrel) is obtained from the US Energy Information Administration ([45]. We compute weekly average of WTI crude oil price, P', between January 13, 2020, and August 25, 2020. We normalize weekly WTI crude oil price P'_t in week t as

$$P_t = \frac{P'_t - \mu_{P'}}{\sigma_{P'}}, \tag{5}$$

where, $\mu_{P'}$ and $\sigma_{P'}$ are the mean and standard deviation of P' between January 13, 2020, and August 25, 2020.

Apple mobility data are obtained from Apple mobility trends reports [2]. The air mobility index is based on two types of data: airline On-Time Performance Data and airport coordinate data. The flight data are obtained from the Bureau of Transportation Statistics (BTS) [5]. And, US airport coordinate data are obtained from a geospatial data management platform named Koordinates [27]. We obtain US COVID-19 data from *Our World in Data* [31].

4 Methodology

We evaluate the impact of driving trends and air mobility on WTI crude oil prices. First, we apply the quantile regression methodology to evaluate the effects of driving trends and air mobility volume on WTI crude oil price. Second, we quantify the left tail or extreme lower quantiles of the WTI crude oil price associated with the COVID-19 pandemic with nonstationary extreme value models.

4.1 Causality

To assess potential predictive utilities of driving trends and air mobility on WTI crude oil price, we use the concept of linear Granger causality [65]. Clearly, nonlinear Granger causality tests [80–82] are another alternative. However, these nonlinear tests require substantially large data than available in our study.

The Granger causality test evaluates whether one time series, X, is useful in forecasting another, time series, Y. In particular, Granger causality investigates whether given information on the past of Y the past of X can deliver any new information that can be used for predicting future Y. To evaluate the causality of X to Y we fit two models, where one model includes X and the other does not include X (base model). Then the predictive performances of these two models are compared to assess causality of X to Y using an F-test, under the null hypothesis of no predictive effect in X to Y (i.e., X does not Granger cause Y), $Var(e_t) = Var(\tilde{e}_t)$.

$$y_t = \alpha_0 + \sum_{k=1}^{d} \alpha_k y_{t-k} + \sum_{k=1}^{d} \beta_k x_{t-k} + e_t, \tag{6}$$

versus the base model

$$y_t = \alpha_0 + \sum_{k=1}^{d} \alpha_k y_{t-k} + \tilde{e}_t. \tag{7}$$

If $Var(e_t)$ is significantly lower than $Var(\tilde{e}_t)$, then x contains additional information that can improve forecasting of y, i.e., X is said to Granger cause Y, which can be denoted by $G_{X \rightarrowtail Y}$, where $\rightarrowtail$ represents the direction of causality [16].

4.2 Quantile Regression

Quantile regression is a generalization of linear regression. Whereas the classical least squares regression estimates the conditional mean of the response variable, quantile regression estimates the conditional median and other quantiles of the response variable. That is, quantile regression constructs a set of regression lines for different quantiles of the conditional distribution of the dependent variable. Unlike least squares regression, quantile regression does not depend on the particular parametric assumption for the dependent variable and it also avoids constant variance assumption [21, 25, 28, 30].

We can model a τth quantile of a response variable y given a particular value of the predictor variable, $\mathbf{X} = \mathbf{x}$, as

$$Q_Y(\tau|\mathbf{x}) = \beta_0(\tau) + \beta_1(\tau)x_1 + \beta_2(\tau)x_2, \tag{8}$$

where $\tau \in (0, 1)$, Y stands for weekly WTI crude oil price (P), X_1 is driving trend (H), and X_2 is air mobility (K^w) [29].

The parameters can be estimated by solving the equation

$$\hat{V}(\tau) = \operatorname*{argmin}_{b} \sum_{i=1}^{n} \rho_\tau(y_i - x_i^T b),$$

where,

$$\rho_\tau(z) = \begin{cases} \tau z, & \text{if } z \geq 0, \\ (\tau - 1)z, & \text{if } z < 0. \end{cases}$$

4.3 Extreme Value Model

Extreme value models evaluate the tail of a distribution and they have a wide range of applications in climate and atmospheric science to industrial risks, geosciences, finance, economics, and insurance [6, 7, 9, 11, 15, 33, 35, 40].

For a sequence of independent random variables, $Y_1, Y_2, ..., Y_n$, with a common distribution function G, let $M_n = \max\{Y_1, Y_2, ..., Y_n\}$ be the maximum of the process over n time units (i.e., *block*) of the observations. For $\{a_n > 0\}$ and $\{b_n\}$ then $Pr\{(M_n - b_n)/a_n \leq z\} \rightarrow G(z)$ as $n \rightarrow \infty$, where G is a non-degenerate function. According to the Fisher and Tippett extremal theorem [22], G belongs to the family of generalized extreme value (GEV) distribution. The distribution function of a non-stationary GEV model can be written as

$$F(z; \mu(t), \sigma(t), \xi(t)) = \exp\left\{-\left[1 + \xi(t)\left(\frac{z - \mu(t)}{\sigma(t)}\right)^{-\frac{1}{\xi(t)}}\right]\right\}, \tag{9}$$

The GEV parameters $\mu(t)$, $\sigma(t)$, and $\xi(t)$ are functions of time or/and other covariates. The t denotes the time (e.g., months, year, etc.) over which the maximum is

chosen. More detail on the non-stationary GEV model can be found in can be found in [10, 13]. The r-year return level, i.e., the level expected to be exceeded once every r year, can be defined as

$$z_r = \mu(t) + \frac{\sigma(t)}{\xi(t)} \left[\left(-\log\left(1 - r^{-1}\right) \right)^{-\xi(t)} - 1 \right]. \tag{10}$$

The return period of a particular extreme event is the inverse of the probability that the event will be exceeded in any given year, i.e., the r-year return level is associated with a return period of r-years.

If $\mu(t) = \mu$, $\sigma(t) = \sigma$ and $\xi(t) = \xi$, the non-stationary GEV model becomes stationary GEV model. We can estimate the GEV model parameters using maximum likelihood estimation (MLE). The concept of return period and return level is used to quantify the likelihood of extreme events.

In our study, we are interested in modeling the lower tail of the WTI crude oil price, P, to evaluate the impact of social distancing and mobility restrictions (i.e., ADI and AMI) on it. That is, we focus on the minima of WTI crude oil price over blocks rather than its maxima. The same GEV model settings can be applied here based on the relation,

$$M_n' = \min\{Y_1, Y_2, ..., Y_n\} = -\max\{-Y_1, -Y_2, ..., -Y_n\}. \tag{11}$$

By rearranging, we find

$$-M_n' = -\min\{Y_1, Y_2, ..., Y_n\} = \max\{-Y_1, -Y_2, ..., -Y_n\}. \tag{12}$$

Therefore, to evaluate the lower tail of WTI crude oil price we use the GEV model on negative block minima of WTI crude oil price [23].

5 Results

In this section, we evaluate the effect of mobility restrictions and social distancing due to COVID-19 on WTI crude oil price. To quantify mobility restrictions and social distancing we use Apple's driving trend index and the newly proposed Air mobility index.

Figure 3 depicts the dynamics of WTI crude oil price, Apple's driving index, and air mobility index from January 2020 to September 2020. It is clear from the figure that the driving trends and air mobility significantly decreased in March and April of 2020, primarily due to the surge of COVID-19 and related stay-at-home orders at different states in the USA during that period. Although the driving trend increased significantly after restrictions eased, air mobility did not increase much primarily because of people's tendency to avoid public transportation. WTI crude oil price gradually increased after lockdown and other restrictions were relaxed.

Now we investigate the potential causality of driving trends and air mobility on the WTI crude oil price. Table 1 presents a summary of the Granger causality tests. We find

Fig. 3 Time plots of normalized weekly average crude oil price ($ per Barrel) and normalized weekly average mobility metrics from January 2020 to August 2020
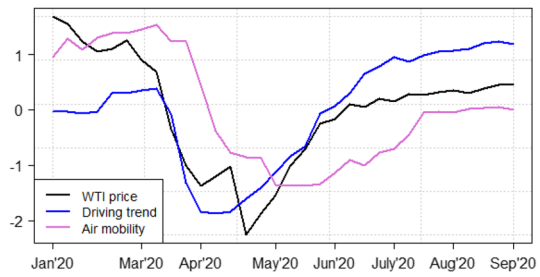

Table 1 Granger Causality among annual WTI crude oil price (Y) and different exogenous variables. The p-value values of the corresponding F-test are given

Causality	Lag 1	Lag 2	Lag 3
Driving trend $\rightarrowtail Y$	0.10*	0.10*	0.26
Air mobility $\rightarrowtail Y$	0.02**	0.19	0.10*

*** $p < 0.01$, ** $p < 0.05$, * $p < 0.10$

that driving trends and air mobility have significant predictive impacts on WTI crude oil price in more than one lag. That is, driving trends and air mobility significantly influence crude oil price formation.

We also develop a quantile regression model for each of the quantiles $\tau = (0.01, 0.05, 0.1, 0.5, 0.9, 0.95, 0.99)$ based on Eq. 9. We are particularly interested in the lower and upper quantiles of the WTI crude oil price. Table 2 summarizes the outputs of the quantile regression models.

We find that both driving trends and air mobility significantly affect lower and upper quantiles as well as the median of the WTI crude oil price. The coefficients of driving trends and air mobility are all positive. Therefore, a decrease (increase) in driving trends or air mobility leads to a decrease (increase) in τ^{th} quantiles of the WTI crude oil price, where $\tau \in (0.01, 0.05, 0.1, 0.5, 0.9, 0.95, 0.99)$. Notice that the coefficient of driving trends tends to gradually decrease from the lower quantiles to the upper quantiles. On the other hand, the coefficient of air mobility tends to gradually increase from the lower quantiles to the upper quantiles. Figure 4 depicts the regression lines of WTI crude oil price for different quantiles.

Now we turn our analysis to evaluate the crash of WTI crude oil price resulting from the COVID-19 pandemic based on the extreme value model. We study monthly minimum crude oil price (Y) for the last twenty years from 2000 to 2020 and model left tail, i.e., extreme lower quantile of the WTI crude oil price. However, due to the unavailability of Apple's driving trends index, we only use monthly air mobility K^m as a covariate in the extreme value modeling. Figure 5 shows the time plot of monthly minimum crude oil price and monthly air mobility (on the 15th of every month) in the USA from January 2000 to August 2020.

We experiment a set of non-stationary extreme value models, $Y'_t \sim GEV(\mu(t), \sigma(t), \xi(t))$, where $Y'_t = -Y_t$, Y_t is the monthly minimum crude oil price in month t. We assess the different combinations of time trends and covariate (air mobility) effect

Table 2 Estimates of quantile regression models for crude oil price with standard errors

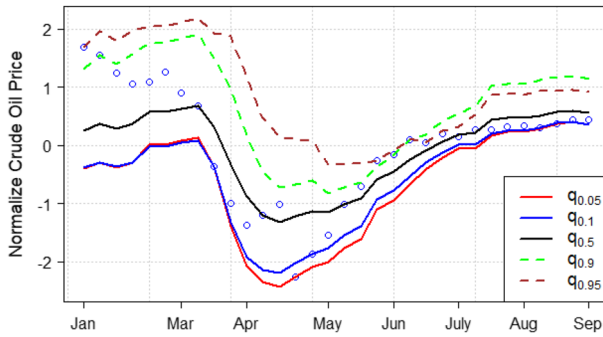| | Quantile (τ) | | | | | | |
	0.01	0.05	0.10	0.50	0.90	0.95	0.99
Constant (β_0)	−0.649***	−0.649***	−0.568***	−0.071	0.405***	0.585***	0.585***
	(0.041)	(0.097)	(0.114)	(0.185)	(0.102)	(0.144)	(0.074)
Driving trends (β_1)	0.846***	0.846***	0.786***	0.527***	0.559***	0.273*	0.273*
	(0.034)	(0.081)	(0.090)	(0.178)	(0.151)	(0.229)	(0.169)
Air mobility (β_2)	0.298***	0.297**	0.229*	0.358**	0.514***	0.617***	0.617***
	(0.077)	(0.145)	(0.170)	(0.199)	(0.085)	(0.088)	(0.039)

*** $p < 0.01$, ** $p < 0.05$, * $p < 0.1$

Fig. 4 Normalized WTI crude oil prices regression models for different quantile levels
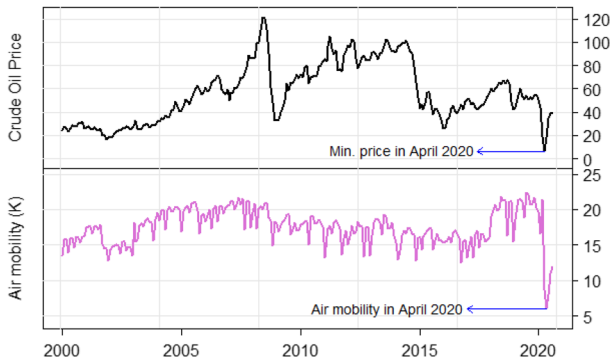

Fig. 5 Monthly minimum crude oil price and monthly air mobility from January 2000 to August 2020

on the monthly minimum crude oil price. We select two best models based on (smaller) Akaike Information Criterion (AIC) [1] and Bayesian information criterion (BIC) [36] values. Table 3 describes the selected models along with a baseline stationary model. Model 1 allows a linear time trend in the location parameter. In Model 2 the location parameter depends linearly on time trend and air mobility. There is a time trend in the log-scale parameter in both models.

Table 3 Different stationarity/non-stationary models with corresponding AIC and BIC

Model	Model descriptions	AIC/BIC
Model 0	$Y_t' \sim GEV(\mu, \sigma, \xi)$	$AIC = 2285.212$
(Stationary)		$BIC = 2295.751$
Model 1	$Y_t' \sim GEV(\mu(t), \sigma(t), \xi)$	$AIC = 2164.935$
	$\mu(t) = \beta_0 + \beta_1 t$	$BIC = 2182.503$
	$\log \sigma(t) = \gamma_0 + \gamma_1 t$	
Model 2	$Y_t' \sim GEV(\mu(t), \sigma(t), \xi)$	$AIC = 2129.58$
	$\mu(t) = \beta_0 + \beta_1 t + \delta K^m$	$BIC = 2150.66$
	$\log \sigma(t) = \gamma_0 + \gamma_1 t$	

Table 4 Estimated parameters of nonstationary GEV models described in Table 3, standard errors are in parenthesis

	$\hat{\beta}_0$	$\hat{\beta}_1$	$\hat{\delta}$	$\hat{\gamma}_0$	$\hat{\gamma}_1$	$\hat{\xi}$
Model 1	−22.11	−0.387		1.974	0.010	−0.606
	(0.651)	(0.014)		(0.056)	(< 0.001)	(0.0443)
Model 2	−27.965	−0.298	−5.190	2.035	0.008	−0.631
	(0.909)	(0.015)	(0.974)	(0.053)	(< 0.001)	(0.049)

Table 4 shows the estimated parameters of Model 1 and Model 2. Notice that, we model negative block minima of WTI crude oil price $(-Y_t)$ and in Model 2 the covariate air mobility has a negative effect on monthly minimum WTI crude oil price, where the estimated value of δ is -5.190, with a standard error of 0.974. That is an increase in air mobility results in an increase in overall WTI crude oil price.

Figure 8 in Appendix represents the goodness of fit plots of the two models. We find that the Quantile–Quantile (Q-Q) plots for both Model 1 and Model 2 are approximately 45-degree line. The density plot of the empirical data suggests that a mixture model would be more adequate. However, since we are mainly interested in modeling the tail (lower) of the distribution, we prefer to consider GEV models. The observed versus fitted density plots suggest a good fit for both Model 1 and Model 2.

Now we evaluate the return level of WTI oil price z_r (i.e., the extreme lower quantile of WTI crude oil price which is expected to fall below on average once every r year) using Eq. 10. Notice that, Model 1 return levels depend on time t. However, Model 2 return levels depend on time t as well as on monthly air mobility. Table 5 provides WTI oil price return levels for two scenarios of the covariates. First, we compute return levels for covariates values in a normal period (January 2016) and then we compute the return levels based on covariates values in a COVID-19 pandemic period (April 2020).

Based on Model 1, for t corresponds to January 2016, the 10-year return level is 42.042, that is, the crude oil price is expected to fall below 42.042 once every 10 years. However, for t corresponds to April 2020 (a day in the COVID-19 pandemic period) this return level fall dramatically to 27.826. Similar outputs are seen for 20, 50, and

Table 5 Estimated WTI oil price return levels

	Covariates values	10-yr return level	20-yr return level	50-yr return level	100-yr return level
Model 1	$t = 193$ (Jan 2016)	42.042	35.387	30.139	27.754
	$t = 244$ (Apr 2020)	27.826	17.049	8.5499	4.687
Model 2	$t = 193$, $K^m = 15308$ (Jan 2016)	35.253	29.911	25.779	23.939
	$t = 244$, $K^m = 8643$ (Apr 2020)	12.687	4.517	−1.801	−4.615

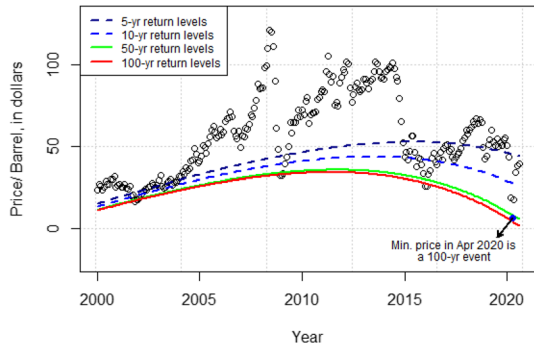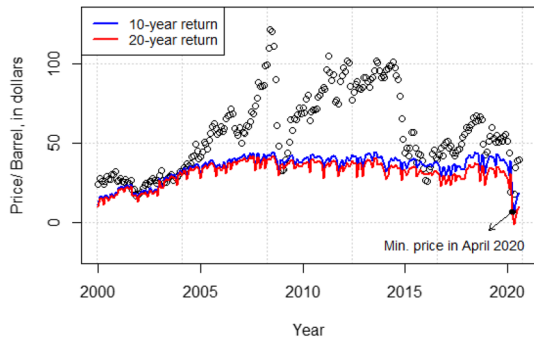**Fig. 6** Return levels of minimum crude oil prices for different return periods, based on Model 1

Fig. 7 Return levels of minimum crude oil prices for different return periods, based on Model 2

100 years return levels. The minimum crude oil price in April 2020 was 6.65 and we find that the 100-year return level is 4.687. Therefore, based on Model 1, we can say that the minimum oil price in April 2020 is a 100-year event, which is also clear in Figure 6.

Now we compute return levels based on Model 2, where we include monthly air mobility as an additional covariate. We find that for the covariates (t and K^m) values in January 2016 the 10 years return level is 12.687. And this value slumps to 12.687 for covariates values in April 2020. That is, lower air mobility increases the risk of occurring a very low oil price. We also find that Model 2 predicts 50-yr return and 100-yr return levels as -1.801 and -4.615, respectively. Therefore, there is a risk of occurring a negative oil price -1.801 in every 50 years, and a negative oil price -4.615 in every 100 years, if there is very low air mobility, i.e., $K^m = 8643$ (with a time trend $t = 244$). Therefore, a COVID-19 like a pandemic, which significantly impacts human mobility (i.e., air mobility), can create a negative oil price every 50 years. (For a similar analysis on how COVID-19 influences to occur negative oil see [42].)

For the values of t and K^m in April 2020, the 10 and 20 years return levels are 12.687 and 4.517, respectively. Therefore, lower air mobility (Model 2) makes the minimum oil price in April 2020 a 20-year event. Figure 7 depicts how a very low oil demand (i.e., oil demand in April 2020) causes frequent lower oil prices.

6 Conclusion

In this paper, we evaluate mobility restrictions and social distancing as determinants of crude oil price collapse during the COVID-19 pandemic. We develop a new air mobility index based on a temporal network to quantify air mobility. Our analysis also demonstrates the impact of the lower driving trends on crude oil prices based on Apple's driving trends index. Based on quantile regression modeling, we find that both driving trends and air mobility significantly affect all quantiles of the WTI crude oil price. On the basis of extreme value modeling, we find that there is a risk of occurring a negative oil price if there is very low air mobility.

Appendix

see Fig. 8.

(a) Q – Q plot for Model 1.

(b) Density plot, Model 1.

(c) Q – Q plot for Model 2.
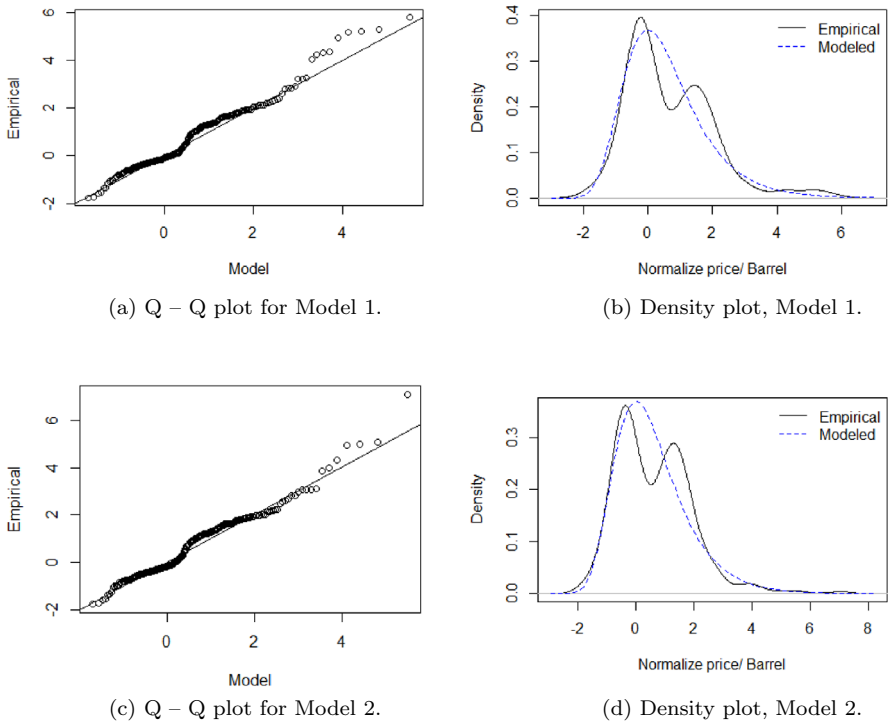
(d) Density plot, Model 2.

Fig. 8 Diagnostic plots for Model 1 and Model 2

References

1. Akaike H (1973) Information theory and an extension of the maximum likelihood principle, Proceedings of the 2nd International Symposium on Information Theory, 267-281
2. Apple (2020) Mobility trends reports, https://covid19.apple.com/mobility, accessed Nov 20, 2020
3. Battiston S, Glattfelder J, Garlaschelli D, Lillo F, Caldarelli G (2010) The structure of financial networks, network science: complexity in nature and technology. Springer, London
4. Abda Emam (2020) The impacts of Covid-19: an econometric analysis of crude oil prices and rice prices in the World. Alinteri J Agri Sci 35:137–143
5. Bureau of Transportation Statistics (BTS) (2020) Reporting Carrier On-Time Performance (1987-present), https://www.transtats.bts.gov/, accessed Nov 20, (2020)
6. Castro-Camilo D, de Carvalho M, Wadsworth J (2018) Time-varying extreme value dependence with application to leading European stock markets. Ann Appl Stat 12(1):283–309
7. Castillo E, Hadi A, Balakrishnan N, Sarabia J (2005) Extreme value and related models with applications in engineering and science, 0-471-67172-X
8. Charoenwong B, Kwan A, Pursiainen V (2020) Social connections with COVID-19-affected areas increase compliance with mobility restrictions. Sci Adv 6(47):eabc3054
9. Chen S, Chai L, Xu K, Wei Y, Rong Z, Wan W (2019) Estimation of the occurrence probability of extreme geomagnetic storms by appling extreme value theory to Aa index. J Geophys Res: Space Phys 124:9943
10. Coles S (2001) An introduction to statistical modeling of extreme values. Springer, Berlin
11. Das K, Dey AK (2016) Quantifying the risk of extreme aviation accidents. Physica A: Statist Mech Appl 463:345–355
12. Demirel G, Barter E, Gross T (2017) Dynamics of epidemic diseases on a growing adaptive network. Sci Rep 7:1–15
13. Dey AK, Edwards A, Das K (2020) Determinants of high crude oil price: a nonstationary extreme value approach. J Statist Theory Pract 14:1–14
14. Dey AK, Haq T, Das K, Panovska I (2020) Quantifying the impact of COVID-19 on the US stock market: An analysis from multi-source information, arXiv:2008.10885
15. Dey AK, Das K (2016) Modeling extreme hurricane damage using the generalized pareto distribution. Am J Math Manag Sci 35:55–66
16. Dey AK, Akcora CG, Gel YR, Kantarcioglu M (2020) On the role of local blockchain network features in cryptocurrency price formation. Can J Statist 48:561–581
17. Energy Information Administration (EIA) (2020) Demand for jet fuel in the U.S. is recovering faster than in many other markets, Washington, DC, USA, https://www.eia.gov/todayinenergy/detail.php?id=44996, accessed Nov 20, 2020
18. Energy Information Administration (EIA) (2020) Spot prices for crude oil and petroleum products, Washington, DC, USA, https://www.eia.gov/dnav/pet/, accessed Nov 20, 2020
19. Enright J, Kao RR (2018) Epidemics on dynamic networks. Epidemics 24:88–97
20. Fang H, Wang L, Yang Y (2020) Human mobility restrictions and the spread of the DNovel Coronavirus (2019-nCoV) in China. J Pub Econ 191:191
21. Fasiolo M, Goude Y, Nedellec R, Wood S (2017) Fast calibrated additive quantile regression. J Am Statist Assoc 116:1402
22. Fisher R, Tippett L (1928) Limiting forms of the frequency distribution of the largest or smallest member of a sample. Math Proc Camb Philos Soc 24(2):180–190
23. Gilleland E, Katz R (2016) extRemes 2.0 an extreme value analysis package in R. J Statist Softw 72(8):1–39
24. Jefferson M (2020) A crude future? COVID-19s challenges for oil demand, supply and prices. Energy Res Soc Sci 68:101669
25. Roger Koenker, Hallock KF (2001) Quantile regression. J Econ Perspect 15(4):143–156
26. Kolaczyk ED, Csárdi G (2014) Statistical analysis of network data with R. Springer, Berlin
27. Koordinates (2020) US airport coordinate, https://koordinates.com/, accessed Nov 20, 2020
28. Koenker R, Xiao Z (2002) Inference on the quantile regression process. Econometrica 70:1583–1612
29. Koenker R (2005) Quantile regression. Econometric society monographs. Cambridge University Press, Cambridge
30. Meinshausen N (2006) Quantile regression forests. J Mach Learn Res 7:983–999
31. Our World (2020) COVID-19 database, https://ourworldindata.org/coronavirus, accessed Nov 20, 2020

32. Pan Y, Darzi A, Kabiri A, Zhao G, Luo W, Xiong C, Zhang L (2020) Quantifying human mobility behaviour changes during the COVID-19 outbreak in the United States. Sci Rep 10(1):20742
33. Reich BJ, Shaby BA (2019) A spatial markov model for climate extremes. J Comput Gr Statist 28(1):117–126
34. Ratti RA, Vespignani JL (2016) Oil prices and global factor macroeconomic variables. Energy Econ 59:198–212
35. Reich BJ, Shaby BA (2012) A Hierarchical max-stable spatial model for extreme precipitation. Annals Appl Statist 6(4):1430–1451
36. Schwarz G (1978) Estimating the dimension of a model. Ananls Statist 6:461–464
37. Setti MO, Voutilainen A (2020) Social distancing with movement restrictions and the effective replication number of COVID-19: multi-country analysis based on phone mobility data, Cold Spring Harbor Laboratory Press, medRxiv: 2020.10.08.20209064
38. Ou S, He X, Ji W, Chen W, Sui L, Gan Y, Lu Z, Lin Z, Deng S, Przesmitzki S, Bouchard J (2020) Machine learning model to project the impact of COVID-19 on US motor gasoline demand. Nat Energy 5(9):666
39. Valdano E, Ferreri L, Poletto C, Colizza V (2015) Analytical computation of the epidemic threshold on temporal networks. Phys Rev X 5(2):021005
40. Wang Z, Jiang Y, Wan H, Yan J, Zhang X (2020) Toward optimal fingerprinting in detection and attribution of changes in climate extremes. Journal of the American Statistical Association. 1-34
41. Zhao L, Wang G, Wang M, Bao W, Li W, Stanley H (2017) Stock market as temporal network. Physica A: Statist Mech Appl 506:1104–1112
42. Corbet S, Goodell JW, Günay S (2020) Co-movements and spillovers of oil and renewable firms under extreme conditions: new evidence from negative WTI prices during COVID-19. Energy Econ 92:104978
43. U.S. Energy Information Administration (EIA), (2018) What drives crude oil prices? USA, U.S, Energy Information Administration (EIA), Washington, DC
44. Energy Information Administration (EIA) (2016) Annual Energy Outlook 2016. USA, U.S, Energy Information Administration (EIA), Washington, DC
45. Energy Information Administration (EIA) (2017) Spot Prices for Crude Oil and Petroleum Products. USA, U.S, Energy Information Administration (EIA), Washington, DC
46. British Petroleum (BP) (2016) BP Statistical Review of World Energy 2016, British Petroleum (BP), London, UK
47. Katz RW, Parlange MB, Naveau P (2002) Statistics of extremes in hydrology. Adv Water Resour 25:1287–1304
48. Edwards AS, Das K (2016) Using statistical approaches to model natural disasters. Am J Undergrad Res 13:87–104
49. Ren F, Giles DE (2010) Extreme value analysis of daily Canadian crude oil prices. Appl Financ Econ 20:941–954
50. Tiakor A, Dey AK, Das K (2017) Predicting Crude Oil Price Using the Non-Stationary Extreme Value Modeling, Joint Statistical Meetings (JSM) Proceedings. Section on Statistical Consulting, Baltimore, MD, pp 2836–2847
51. Ding Y (2018) A novel decompose-ensemble methodology with AIC-ANN approach for crude oil forecasting. Energy 154:328–336
52. Chiu F, Hsu C, Ho A, Chen C (2016) Modeling the price relationships between crude oil, energy crops and biofuels. Energy 109:845–857
53. Fisher RA, Tippett LHC (1928) Limiting forms of the frequency distribution of the largest and smallest member of a sample. Proc Camb Philos Soc 24(2):180–190
54. Caroni C, Panagoulia D (2016) Non-stationary modelling of extreme temperatures in a mountain area of greece. Springer, Berlin
55. OECD (2016) OECD studies on water mitigating droughts and floods in agriculture: policy lessons and approaches on water. OECD Publishing, Paris
56. Pisarenko VF, Sornette A, Sornette D, Rodkin MV (2014) Characterization of the tail of the distribution of earthquake magnitudes by combining the GEV and GPD descriptions of extreme value theory. Pure Appl Geophys 171:1599–1624
57. von Neumann J (1941) Distribution of the ratio of the mean square successive difference to the variance. Ann Math Statist 12(4):367–395

58. Chul-Yong Lee, Sung-Yoon Huh (2017) Forecasting long-term crude oil prices using a bayesian model with informative priors. Sustainability 9:190
59. Risser Mark D, Wehner Michael F (2017) Attributable human-induced changes in the likelihood and magnitude of the observed extreme precipitation during hurricane harvey. Geophys Res Lett 44:457–464
60. Mensah E (2016) Box-Jenkins modelling and forecasting of Brent crude oil price, MPR-online 67748
61. Morana C (2001) A semiparametric approach to short-term oil price forecasting. Energy Econ 23:325–338
62. Mikosch T, Starica C (2004) Nonstationarities in financial time series, the long range dependence, and IGARCH effects. Rev Econ Statist 86:378–390
63. Economou E, Agnolucci P, Fattouh B, De Lipis V (2017) A structural model of the world oil market: the role of investment dynamics and capacity constraints, The Oxford Institute for Energy Studies
64. Nurhadi SR (2016) Value at risk VaR of dynamic crude oil prices for project risk and economics - application of extreme value theory EVT and peak-over-threshold POT Model, Society of Petroleum Engineers
65. Granger CWJ (1969) Investigating causal relations by econometric models and cross-spectral methods. Econometrica 37:424–438
66. Akcora CG, Dey AK, Gel YR, Kantarcioglu M (2018) Forecasting Bitcoin Price with Graph Chainlets. Proc. Advances in Knowledge Discovery and Data Mining (PAKDD), (2018) 765–776. Springer, Cham
67. Gilleland E, Katz RW (2016) extRemes 2.0: an extreme value analysis package in R. J Statist Softw 72(8):1–39
68. Said Said E, Dickey DA (1984) Testing for unit roots in autoregressive-moving average models of unknown order. Biometrika 71(3):599–607
69. Maziarz M (2015) A review of the Granger-causality fallacy. J Philos Econ 8(2):86
70. Mannino M, Bressler S (2015) Foundational perspectives on causality in large-scale brain networks. Phys Life Rev 15:107–123
71. Colgan JD (2013) Fueling the fire: pathways from oil to war. Int Secur 38(2):147–180
72. Jaffe AM, Elass J (2015) War and the oil price cycle. J Int Affairs 69(1):121–137
73. Kollias C, Kyrtsou C, Papadamou S (2013) The effects of terrorism and war on the oil price-stock index relationship. Energy Econ 40:743–752
74. Barrell R, Delannoy A, Holland D (2011) The impact of high oil prices on the economy. Natl Inst Econ Rev 217:F68–F74
75. Blanchard OJ, Gali J (2007) The macroeconomic effects of oil shocks: why are the 2000s so different from 1970s, NBER Working Paper No. 13368
76. Sill K (2007) The macroeconomics of oil shocks. Bus Rev, Federal Reserve Bank Phila Q1:21–31
77. Narayan PK (2020) Oil price news and COVID-19–Is there any connection? Energy Res Lett 1(1):1–5
78. Akhtaruzzaman Md, Boubaker S, Chiah M, Zhong A (2020) COVID19 and oil price risk exposure. Financ Res Lett 2020:101882
79. Mugaloglu E, Polat AY, Tekin H, Dogan A (2021) Oil price shocks during the COVID-19 pandemic: evidence from United Kingdom energy stocks. Energy Res Lett 2(1):24253
80. Hiemstra C, Jones J (1994) Testing for linear and nonlinear granger causality in the stock price- volume relation. J Financ 49(5):1639–1664
81. Diks C, Panchenko V (2006) A new statistic and practical guidelines for nonparametric granger causality testing. J Econ Dyn Control 30(9):1647–1669
82. Alex Tank, Ian Covert, Nicholas Foti, Ali Shojaie, Fox Emily B (2021) Neural Granger Causality. IEEE Transactions on Pattern Analysis and Machine Intelligence. https://doi.org/10.1109/TPAMI.2021.3065601